

Wigner Function For A Kerr State

Magdalena Stobińska*

Instytut Fizyki Teoretycznej, Uniwersytet Warszawski, Warszawa 00-681, Poland

G. J. Milburn

*Centre for Quantum Computer Technology and School of Physical Sciences,
The University of Queensland, St Lucia, Queensland 4072, Australia*

Krzysztof Wódkiewicz†

Instytut Fizyki Teoretycznej, Uniwersytet Warszawski, Warszawa 00-681, Poland

Department of Physics and Astronomy, University of New Mexico, Albuquerque, NM 87131-1156, USA
(Dated: February 7, 2019)

We present numerical simulations of the Wigner function for a one-mode Kerr state. A Kerr state is a quantum squeezed state and its Wigner function reveals negativities. This state can be generated using an optical fiber with $\chi^{(3)}$ nonlinearity. However, the nonlinearity is too small to reach the regime of evolution where the negativities of the Wigner function are present. We discuss a scheme to generate Kerr states in an ion trap and show how the negative Wigner functions can be measured. The production scheme involves 10 laser pulses and it seems to be achievable with a current technology.

I. INTRODUCTION

In this article we study the Wigner function for a one-mode squeezed nongaussian state, a Kerr state. This state can be produced using a photon coherent state interacting with $\chi^{(3)}$ nonlinearity in the optical fibre. This is a highly nonclassical state and after a certain time of evolution in the fibre its Wigner function would take negative values in the phase space. However the nonlinearity in a fibre is too small to reach a highly nonlinear regime and thus produces the negativity in an experimentally reasonable time.

The Kerr state can also be obtained via vibronic motion engineering in ion traps which simulates the generation of a Kerr state with an arbitrarily long time of evolution or arbitrarily high nonlinearity in the fibre. Trapped ions seem to be a promising implementation. Even though their make-up is complicated and includes many degrees of freedom, both internal (electronic) and external (vibronic), a simple theory developed for traditional quantum optical systems consisting of photons and single atoms, is still applicable: For example, a strongly confined trapped ion coupled to an electromagnetic field is well described by the Jaynes and Cummings model.

We show that a measurement of the Wigner function for the Kerr state of an ion's vibrational motion could be performed using currently available technology.

II. ONE-MODE SQUEEZED KERR STATE

The interaction Hamiltonian for a totally degenerate four-wave mixing process in an optical fiber with no losses is of second-order in creation a^\dagger and annihilation a operators

$$H = \hbar \frac{\kappa}{2} a^\dagger a^\dagger a a, \quad (1)$$

where κ is a nonlinear constant proportional to $\chi^{(3)}$. A one-mode squeezed Kerr state results from an action of a unitary evolution operator $U_K(\tau) = \exp \left\{ \frac{-iHt}{\hbar} \right\}$ on a coherent state $|\alpha\rangle$

$$|\Psi_K(\tau)\rangle = U_K(\tau)|\alpha\rangle = \exp \left\{ i \frac{\tau}{2} a^\dagger a^2 \right\} |\alpha\rangle, \quad (2)$$

where $\tau = -\kappa t$ is a unitless parameter and t is the evolution time in a Kerr medium. The value of this parameter determines whether the state is Gaussian or not. The Kerr state (2) can be expressed in the Fock state basis in the following way

$$|\Psi_K(\tau)\rangle = e^{-\frac{|\alpha|^2}{2}} \sum_{n=0}^{\infty} \frac{\alpha^n}{\sqrt{n!}} e^{i\frac{\tau}{2}n(n-1)} |n\rangle. \quad (3)$$

For $\tau = 0$ this expansion reduces to the coherent state $|\alpha\rangle$.

The Kerr state is a squeezed state for certain values of the parameter τ with Poissonian photon statistics: the second-order coherence function is constant in time, $g^{(2)}(\tau) = 1$. The statistics remain unchanged under evolution in the Kerr medium because the mean number of photons is a constant of motion. The second-order moments for the state are the following

$$\langle a^\dagger a \rangle = |\alpha|^2, \quad \langle a^2 \rangle = \alpha^2 e^{i\tau + |\alpha|^2 (e^{2i\tau} - 1)}. \quad (4)$$

*Electronic address: magda.stobinska@fuw.edu.pl

†Electronic address: wodkiew@fuw.edu.pl

Unlike for Gaussian states, they do not specify the state completely therefore higher-order moments have to be also known.

The nonlinear refractive index $n(\alpha)$ of Kerr medium is intensity dependent

$$n(\alpha) = n_0 + n_2 |\alpha|^2. \quad (5)$$

The intensity fluctuations modulate the nonlinear refractive index and this in turn modulates the phase of travelling light. Photons with stronger amplitude will acquire phase faster than photons with smaller amplitude. This effect can be observed by studying the easy-to-compute Q-function evolution

$$Q(\tau, \beta, \beta^*) = \frac{1}{\pi} e^{-(|\alpha|^2 + |\beta|^2)} \left| \sum_n \frac{(\alpha\beta^*)^n}{n!} e^{i\frac{\tau}{2}n(n-1)} \right|^2. \quad (6)$$

Assuming that α is real, the circular shape of the error contour for a coherent state will be placed in the phase space on the real axis, with its center at α . The “part” of the circular shape of error contour for larger values of α will rotate faster than those for smaller α . The circular shape will be first stretched into an ellipse and then into a crescent shape. Therefore, squeezing will not be seen in the principal axes directions but for quadratures at a certain angle [1]. The contour plot of the Q-function is plotted in [2]. Solutions of the Fokker-Planck equation for the Q-function in a dissipative and noisy Kerr medium have been widely studied [2, 4, 5, 6].

The information about nonclassicality of the state can also be obtained from the Wigner function. As is very well known, the Wigner function can be measured experimentally, including its negative values [3]. The Wigner function for the one-mode Kerr state in a nondissipative medium can be evaluated directly using its density operator and expressed in two equivalent ways

$$W(\tau, \gamma, \gamma^*) = \frac{2}{\pi} e^{-2|\gamma|^2} e^{-|\alpha|^2} \sum_{q=0}^{\infty} \frac{(2\alpha^* \gamma e^{i\frac{\tau}{2}})^q}{q!} e^{-i\frac{\tau}{2}q^2} \times \sum_{k=0}^{\infty} \frac{(2\alpha \gamma^* e^{-i\frac{\tau}{2}})^k}{k!} e^{i\frac{\tau}{2}k^2} e^{-|\alpha|^2} e^{i\tau(k-q)}, \quad (7)$$

$$W(\tau, \gamma, \gamma^*) = \frac{2}{\pi} e^{2|\gamma|^2} e^{-|\alpha|^2} \sum_{n,m=0}^{\infty} \frac{1}{(-2)^{n+m}} \frac{\alpha^n}{n!} \frac{\alpha^{*m}}{m!} \times e^{i\frac{\tau}{2}[n(n-1)-m(m-1)]} (\partial_{\gamma})^n (\partial_{\gamma^*})^m e^{-4|\gamma|^2} \quad (8)$$

Figures 1, 2, 3, 4 show the plot of the Wigner function for different parameters τ and times of evolution for $\alpha = 5$. Due to the preserved number of photons, the probability distribution during its evolution will remain situated within at the circle of radius $|\alpha|$. The distribution, beginning from a circular shape, turns into an ellipse and squeezing appears in the appropriate direction. Then the ellipse changes into a banana shape. Squeezing increases and the state becomes nongaussian. For $\tau = \frac{\pi}{2}$

we achieve the Wigner function for a kitten state

$$|\Psi(\tau = \pi/2)\rangle = \frac{1}{2} |5e^{i\frac{\pi}{4}}\rangle - \frac{1}{2} e^{i\frac{\pi}{4}} | - 5e^{-i\frac{\pi}{4}} \rangle + \frac{1}{2} | - 5e^{i\frac{\pi}{4}}\rangle + \frac{1}{2} e^{i\frac{\pi}{4}} |5e^{-i\frac{\pi}{4}}\rangle, \quad (9)$$

where $5e^{i\frac{\pi}{4}} \simeq 3.5 + 3.5i$ and for $\tau = \pi$ we get a cat state

$$|\Psi(\tau = \pi)\rangle = \frac{1}{\sqrt{2}} (e^{-i\frac{\pi}{4}} |5i\rangle + e^{i\frac{\pi}{4}} | - 5i\rangle). \quad (10)$$

This is also known as a fractional revival [7].

Similarly, as for the Q-function an interference pattern can be seen in those plots: a “tail” of interference fringes follows the banana shape of the Wigner function. These fringes arise due to interference of Fock states, which are the building blocks for a Kerr state (3). Its Wigner function can be viewed as a superposition of Wigner functions $W_{|n\rangle\langle n|}(\gamma, \gamma^*)$ for Fock number states $|n\rangle$

$$W(\tau, \gamma, \gamma^*) \simeq \sum_{n=0}^{\infty} \frac{|\alpha|^2 n}{n!} W_{|n\rangle\langle n|}(\gamma, \gamma^*) + f(\tau, \gamma, \gamma^*). \quad (11)$$

Negativities achieved in the Wigner function correspond to zeros of the Q-function [8].

In a general case of a Kerr medium with damping and in presence of thermal noise the dynamics of the Wigner function are governed by the Fokker-Planck equation which takes the following form in the polar basis $\gamma = r e^{i\phi}$ with $r = |\gamma|$

$$\partial_{\tau} W(\tau, r, \phi) = \left\{ (r^2 - 1) \partial_{\phi} - \frac{1}{16} \left(\frac{1}{r} \partial_r \partial_{\phi} + \partial_r^2 \partial_{\phi} + \frac{1}{r^2} \partial_{\phi}^3 \right) + \xi + \frac{\xi}{2} \left(r + \frac{1}{2} \left(\frac{1}{2} + N_0 \right) \frac{1}{r} \right) \partial_r + \frac{\xi}{4} \left(\frac{1}{2} + N_0 \right) \left(\partial_r^2 + \frac{1}{r^2} \partial_{\phi}^2 \right) \right\} W(\tau, r, \phi), \quad (12)$$

where $\xi = \sigma/\kappa$, σ is a damping constant and N_0 is a thermal noise. This is a third-order nonlinear differential equation. The first line in it describes the dynamics in the ideal Kerr medium. Note that the first term in it shows that the velocity of rotation depends on the distance from the co-ordinates origin. The next two lines in the equation are present only in case of damping $\xi \neq 0$.

All the figures 1-4 have been obtained by three independent numerical simulations: computing the equations (7), (8) and (12).

To estimate what ranges of parameter τ are available for an optical fiber we notice that $\kappa = \frac{8\pi^2 \hbar \omega^2}{\epsilon_0 n_0^4(\omega) V} \chi^{(3)}$, where ω is the frequency of the injected light beam, $n(\omega)$ is the linear refractive index, V is the volume of quantisation.

For a typical silica fiber $\chi^{(3)} \simeq 10^{-22} \frac{\text{m}^2}{\text{V}^2}$, $n_0(\omega) = 1.46$. For the quantisation volume we take $V = L \cdot A \text{ m}^3$, where $A \simeq 8 \mu\text{m}$ is a typical effective core area for a

single mode fiber and L is the length of coherence. For pulsed light L is just the length of a pulse.

For a radiofrequency $\omega = 10^{13}$ Hz pulsed coherent light of amplitude $|\alpha|^2 = 10^8$ and pulse duration of $t_p = 100$ fs ($L = 0.02$ mm) the value of $\tau = 10^{-8}$ would be achieved for a fiber of length $l = 154 \cdot 10^3$ km (a fiber folded 10 times between Australia and Europe). If we had a fiber of $\chi^{(3)} = 1.5 \cdot 10^{-17} \frac{\text{m}^2}{\text{V}^2}$ we would obtain it for a $l = 1$ km fiber ($t = 0.5 \cdot 10^{-5}$ s). The same value of τ for this fiber would be obtained for $\chi^{(3)} = 1.5 \cdot 10^{-14} \frac{\text{m}^2}{\text{V}^2}$ for longer pulses corresponding to $L = 10$ mm. Microstructured fibers seem to be more promising with $\chi^{(3)} \simeq 10^{-16} \frac{\text{m}^2}{\text{V}^2}$. However their length does not exceed 1m with current technology.

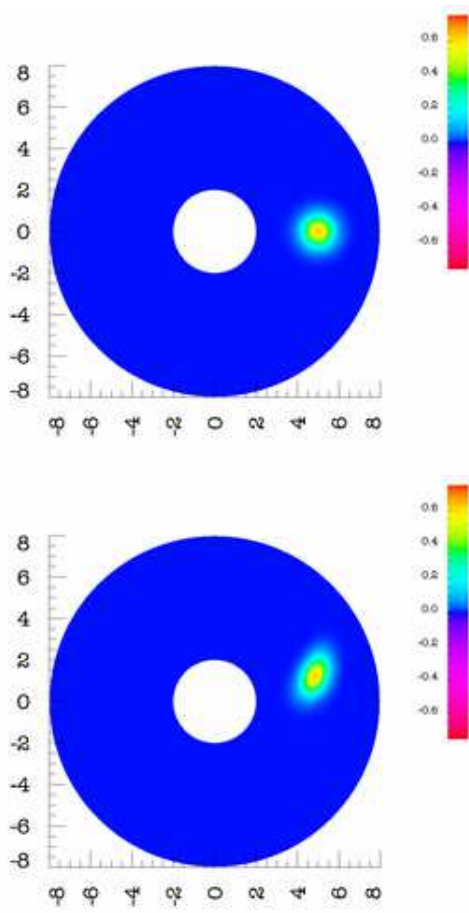


FIG. 1: The Wigner function for $\alpha = 5$ and $\tau = 0$ is a gaussian function for the coherent state - the top figure. Due to the fact that the coefficient for a Kerr state are periodic functions of τ , for $\tau = 2\pi$ we achieve the same shape of the Wigner function. For $\tau = 0.01$ the Wigner function is an ellipse and the state becomes squeezed - the bottom figure.

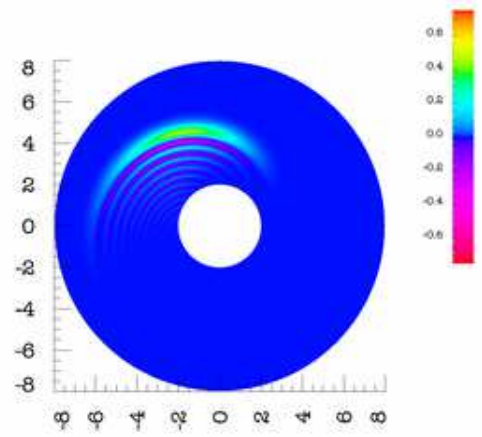
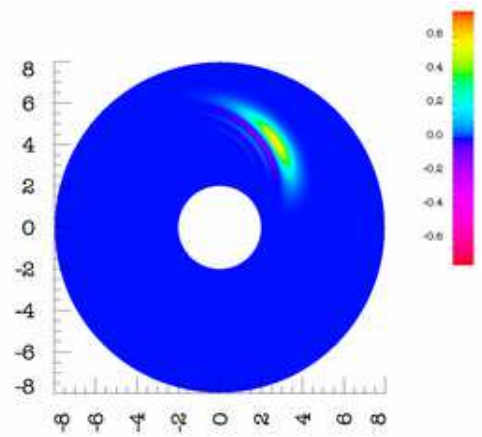


FIG. 2: The Wigner function for $\alpha = 5$ and longer evolution time: $\tau = 0.04$ - the top figure and $\tau = 0.08$ - the bottom figure. The negativities appear and form a tail of interference fringes.

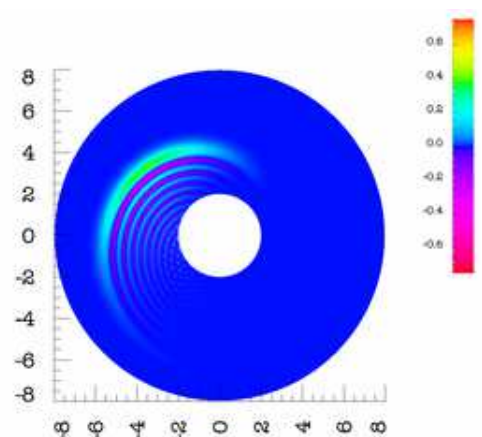


FIG. 3: The Wigner function for $\alpha = 5$ and $\tau = 0.1$.

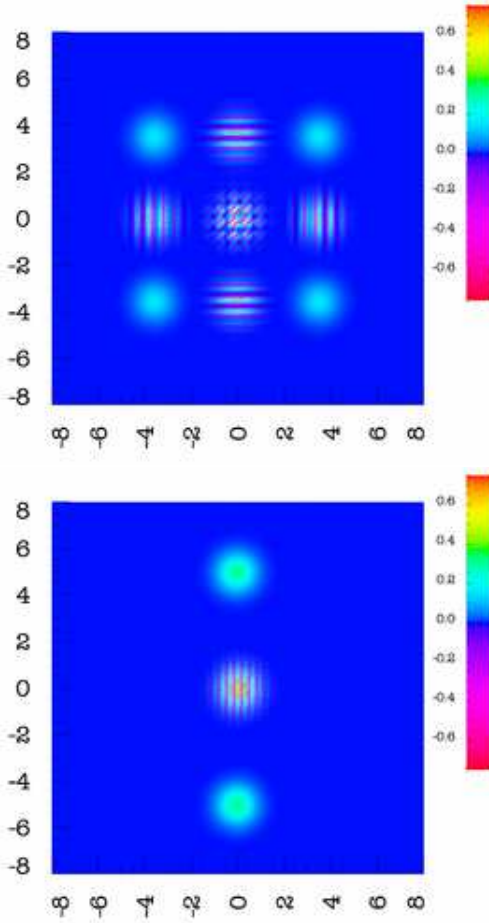


FIG. 4: The Wigner function for $\alpha = 5$ and $\tau = \frac{\pi}{2}$ - the top figure. The Kerr state becomes a superposition of four coherent states: $|5e^{i\frac{\pi}{4}}\rangle, |5e^{-i\frac{\pi}{4}}\rangle, |-5e^{i\frac{\pi}{4}}\rangle, |-5e^{-i\frac{\pi}{4}}\rangle$ which interfere. Similarly for $\tau = \pi$ the Kerr state becomes a cat state: $\frac{1}{\sqrt{2}}(e^{-i\frac{\pi}{4}}|5i\rangle + e^{i\frac{\pi}{4}}|-5i\rangle)$ - the bottom figure. The interference fringes appear in between.

III. ION TRAP

A system consisting of a trapped ion with vibration motion initially prepared in a Kerr state seem to be more feasible for a measurement of the Wigner function. A method of preparing an ion in a Paul trap [9] in an arbitrary state of the following form has been proposed in [10, 11]

$$|\Psi\rangle = \delta|\Psi^e\rangle|e\rangle + \beta|\Psi^g\rangle|g\rangle, \quad (13)$$

where

$$|\Psi^e\rangle = \sum_{n=0}^M w_n^e |n\rangle, \quad |\Psi^g\rangle = \sum_{n=0}^M w_n^g |n\rangle \quad (14)$$

are ion motional states, $|n\rangle$ is a Fock state of a harmonic oscillator potential in the trap, $M < \infty$. $|g\rangle$ and $|e\rangle$ are the ion electronic ground and excited states. The method

is based on applying a series of laser pulses tuned to the carrier frequency and the red sideband of the ion trap alternately. Adjusting the amplitude and phase of each pulse properly, we could achieve $w_n^e = w_n^g = w_n$ equal to

$$w_n = \frac{1}{\sqrt{\sum_{k=0}^M \frac{|\alpha|^{2k}}{k!}}} \frac{\alpha^n}{\sqrt{n!}} e^{i\frac{\pi}{2}n(n-1)}. \quad (15)$$

Those coefficients would correspond to the coefficients of the Kerr state decomposition in Fock basis (3) up to the normalisation factor. This results from the fact that we cut off the infinite sum in (3) and take into account only the first M terms in it.

This method would allow to produce an approximated Kerr state $|\Psi_K^{(M)}(\tau)\rangle$ at an arbitrary long time of evolution τ , even for those values which were not accessible for photons. In this case we would have $|\Psi^e\rangle = |\Psi^g\rangle$. Choosing the value of M we could approximate the Kerr state (3) with an arbitrary good accuracy. In this case the state of ion is given by

$$|\Psi_K^{(M)}(\tau)\rangle = \frac{1}{\sqrt{\sum_{k=0}^M \frac{|\alpha|^{2k}}{k!}}} \sum_{n=0}^M \frac{\alpha^n}{\sqrt{n!}} e^{i\frac{\pi}{2}n(n-1)} |n\rangle \times (\delta|e\rangle + \beta|g\rangle). \quad (16)$$

The number of required pulses for preparing the ion in an approximated Kerr state is equal to $2M + 1$ and the parameters δ and β , though arbitrary, have to be known to arrange them. Choosing one of them equal to $\delta = 0$ and $\beta = 1$ will decrease the number of pulses: $2M$. The value of M is strongly α dependent. The dependence of number of significant w_n for $\alpha = 10$ and $\alpha = 1$ on n is depicted on Fig. 5. Although the number of significant w_n for $\alpha = 10$ is $M = 160$, which corresponds to 320 laser pulses, for $\alpha = 1$ the number is $M = 10$, which means 20 pulses. The latter result seems to be experimentally realisable. Additionally we compare the Wigner function achieved in numerical simulation for the Kerr state $M = \infty$ (3) and for the approximated Kerr state with $M = 5$ and $M = 4$ (16) for $\alpha = 1$ on Fig. 6, 7, 8, 9. $M = 5$ seem to be a good approximation as well and it corresponds to 10 laser pulses. $M = 4$ simplifies the state too much and the Wigner function differs from the Wigner function of original Kerr state significantly.

In that case we would have

$$|\Psi_K^{(5)}(\tau)\rangle = R_5 \cdot \dots \cdot C_1 R_1 C_0 |0, g\rangle, \quad (17)$$

where we use C_j and R_j for an evolution due to the laser at the carrier frequency and red sideband, respectively. In order to generate this state with $\delta = 0$ we assume the carrier resonance Rabi frequency equal to $\Omega_C = 1\text{MHz}$ and the red sideband Rabi frequency equal to $\Omega_R = 100\text{kHz}$. For those frequencies the duration time of pulses are as follows

$$t_0^C = 1.92\mu\text{s}, \quad t_1^R = 0.69\text{ms}, \quad (18)$$

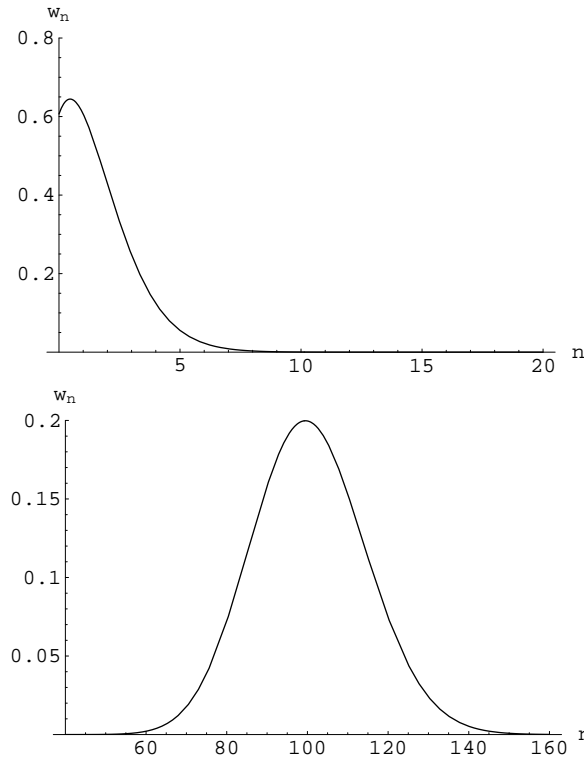


FIG. 5: Kerr state coefficients in Fock basis decomposition as a function of n for $\alpha = 1$ - the upper plot and $\alpha = 10$ - the lower plot.

$$t_1^C = 1.68\mu\text{s}, t_2^R = 0.50\text{ms}, \quad (19)$$

$$t_2^C = 7.35\mu\text{s}, t_3^R = 0.83\text{ms}, \quad (20)$$

$$t_3^C = 2.44\mu\text{s}, t_4^R = 0.36\text{ms}, \quad (21)$$

$$t_4^C = 2.72\mu\text{s}, t_5^R = 0.70\text{ms}. \quad (22)$$

where we assumed the Lamb-Dicke parameter $\eta = 0.02$. Depending on what is more convenient we could keep the duration time of pulses constant and change the Rabi frequencies from pulse to pulse.

Having the ion already prepared we could measure the Wigner function of the vibronic state using either the standard method of quantum tomography [12, 13] or the method of direct measurement of Wigner function developed in [14].

IV. CONCLUSION

We have presented the Wigner function for the Kerr state. This state seems to be a very good approximation of a one-mode gaussian squeezed state for photons due to very small value of nonlinearity in a optical fiber. However we still can reach the nongaussian regime for this state using another system: trapped ion. For an ion we can produce an arbitrary good approximation of the Kerr state. This method can be applied for any other one-mode state and can be developed for two-mode states. It

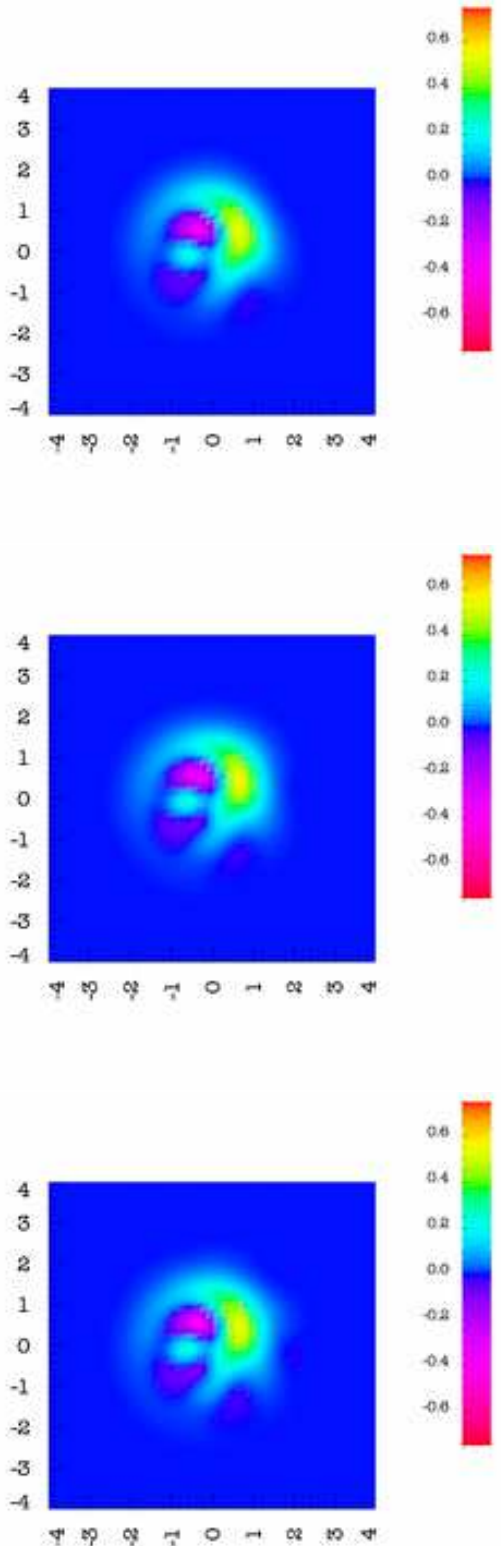


FIG. 6: The Wigner function for $\alpha = 1$ and $\tau = 1$. The top figure for $M = 4$, the middle figure for $M = 5$, the bottom figure for $M = \infty$.

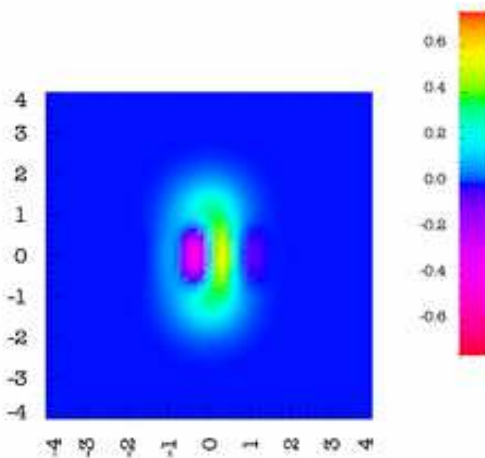
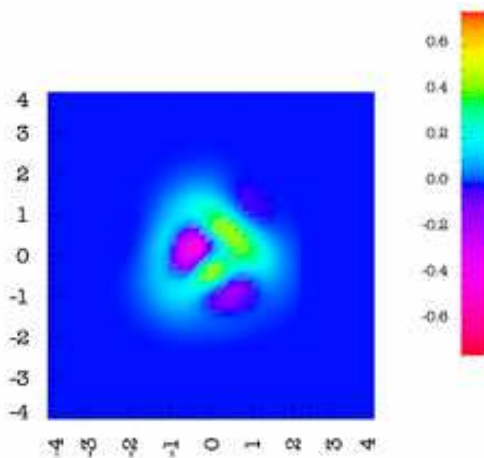
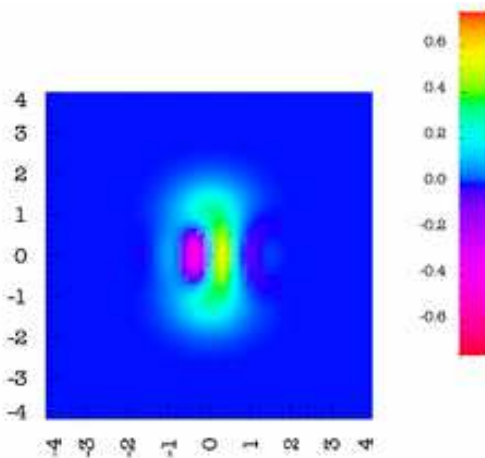
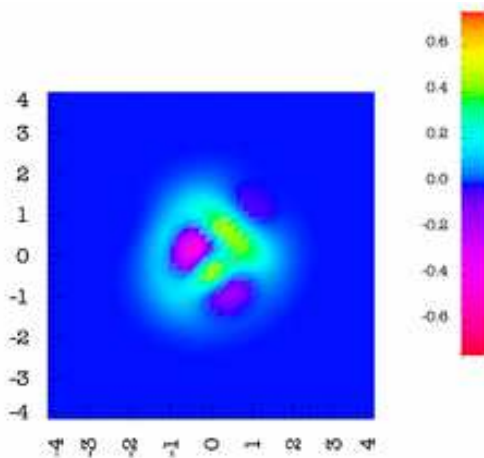
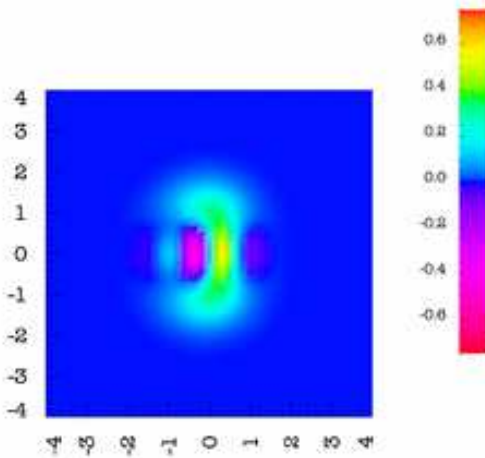
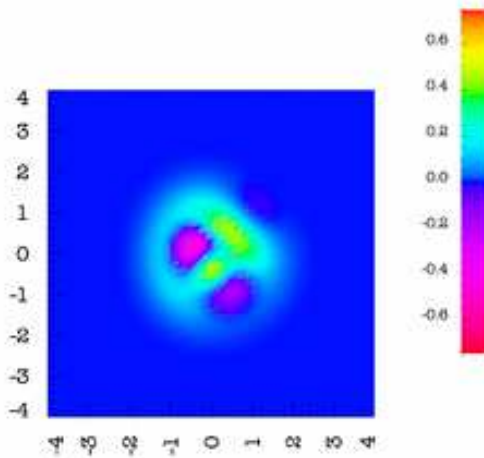


FIG. 7: The Wigner function for $\alpha = 1$ and $\tau = 2$. The top figure for $M = 4$, the middle figure for $M = 5$, the bottom figure for $M = \infty$.

FIG. 8: The Wigner function for $\alpha = 1$ and $\tau = \pi$. The top figure for $M = 4$, the middle figure for $M = 5$, the bottom figure for $M = \infty$.

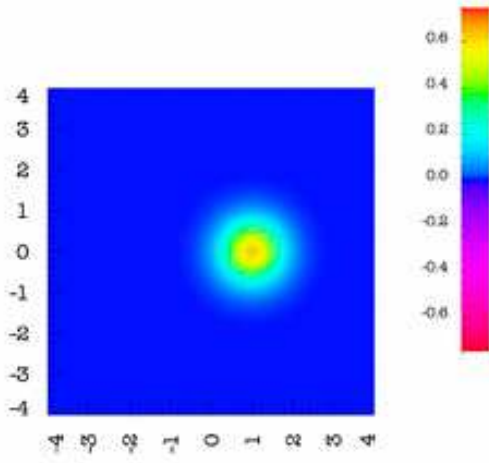
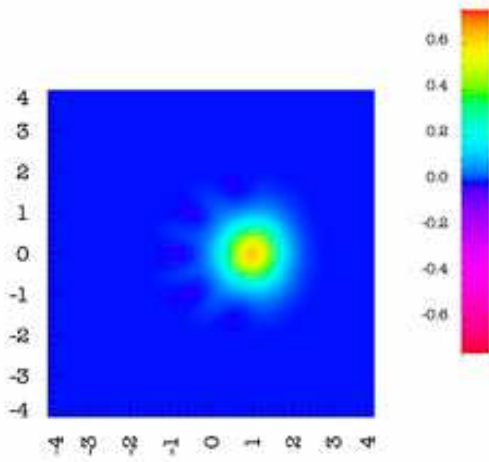
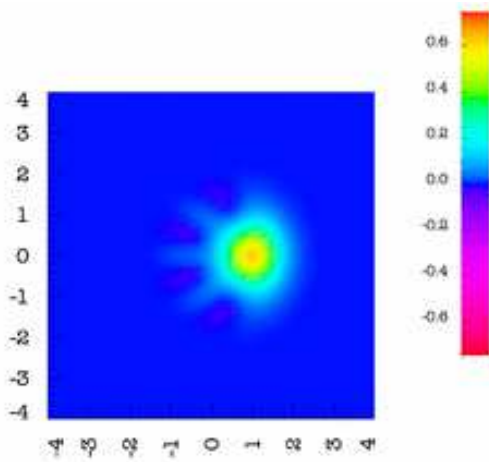


FIG. 9: The Wigner function for $\alpha = 1$ and $\tau = 2\pi$. The top figure for $M = 4$, the middle figure for $M = 5$, the bottom figure for $M = \infty$.

requires solving a set of nonlinear equations which give the amplitudes and phases of the laser pulses.

Acknowledgments

M.S. would like to thank Adam Buraczewski for advising on selection of numerical methods and applying data compression algorithm and Timothy Ralph for his hospitality and stimulating discussions in Brisbane.

This work was partially supported by a MEN Grant No. 1 PO3B 137 30.

[1] H. A. Bachor and T. Ralph, *A Guide to Experiments in Quantum Optics*, (Wiley-Vch, 2004).

[2] R. Tana, *Nonclassical states of light propagating in Kerr media*.

[3] G. Nogues, A. Rauschenbeutel, S. Osnaghi, P. Bertet, M. Brune, J. M. Raimond, S. Haroche, L. G. Lutterbach, and L. Davidovich, Phys. Rev. A **62**, 054101, (2000).

[4] G. J. Milburn and C. A. Holmes, Phys. Rev. Lett. **56**, 2237, (1986).

[5] D. J. Daniel and G. J. Milburn, Phys. Rev. A **39**, 4628, (1989).

[6] V. Perinova and A. Luks, Phys. Rev. A **41**, 414, (1990).

[7] I. Sh. Averbukh and N. F. Perelman, Phys. Let. **139**, 449 (1989).

[8] H. J. Korsch, C. Muller, and H. Wiescher, J. Phys. A **30**, L677 (1997).

[9] D. Leibfried, R. Blatt, C. Monroe, and D. Wineland, Rev. Mod. Phys. **75**, 281, (2003).

[10] S. A. Gardiner, J. I. Cirac, and P. Zoller, Phys. Rev. A **55**, 1683, (1997).

[11] B. Kneer and C. K. Law, Phys. Rev. A **57**, 2096, (1998).

[12] S. Wallentowitz and W. Vogel, Phys. Rev. Lett. **75**, 2932, (1995).

[13] J. F. Poyatos, R. Walser, J. I. Cirac, and P. Zoller, Phys. Rev. A **53**, (1996).

[14] L. G. Lutterbach and L. Davidovich, Phys. Rev. Lett. **78**, 2547, (1997).